

Lawrence Berkeley National Laboratory

Lawrence Berkeley National Laboratory

Title

Multiphonon Resonance Raman Scattering in InGaN

Permalink

<https://escholarship.org/uc/item/8wq5r37w>

Authors

Ager III, J.W.
Walukiewicz, W.
Shan, W.
[et al.](#)

Publication Date

2005-06-28

Peer reviewed

Multiphonon Resonance Raman Scattering in InGaN

J. W. Ager III ^{a)}, W. Walukiewicz^{a)}, W. Shan ^{a)}, K. M. Yu ^{a)}, S. X. Li, ^{a),b)} E. E. Haller ^{a),b)},
H. Lu ^{c)}, and W. J. Schaff ^{c)}

^{a)} Materials Sciences Division, Lawrence Berkeley National Laboratory, Berkeley,
California 94720

^{b)} Department of Materials Science and Engineering, University of California, Berkeley,
California 94720

^{c)} Department of Electrical and Computer Engineering, Cornell University, Ithaca, New
York 14853

PACS: 78.30.Fs, 78.66.Fd, 63.20.-e

ABSTRACT

In $\text{In}_x\text{Ga}_{1-x}\text{N}$ epitaxial films with $0.37 < x < 1$ and free electron concentrations in the 10^{18} cm^{-3} range, strong resonant Raman scattering of $A_1(\text{LO})$ phonon is observed for laser excitation in Raman scattering when excited above the direct band gaps. Examination of films with direct band gaps between 0.7 and 1.9 eV using laser energies from 1.9 to 2.7 eV shows that the resonance is broad, extending to up to 2 eV above the direct gap. Multiphonon Raman scattering with up to 5 LO phonons is also observed for excitation close to resonance in alloy samples; this is the highest number of phonon overtones ever observed for multiphonon scattering in a III-V compound under ambient conditions. Coupling of the electron plasmon to the LO phonon to form a longitudinal plasmon coupled mode of the type which is observed in the Raman spectra of n-GaN, appears not to occur in $\text{In}_x\text{Ga}_{1-x}\text{N}$ for $x > 0.37$.

INTRODUCTION

InN and In-rich nitrides have been less well studied than GaN, AlN, and their alloys. However, there is increased interest in these materials, particularly after the recent discovery that InN has a relatively narrow gap of 0.7 eV [1,2,3]. Raman studies of III-V nitrides have been reviewed recently by Harima [4]. For hexagonal nitrides in the $z(y,y)\bar{z}$ backscattering geometry the E_2 (low and high) and $A_1(\text{LO})$ zone-center phonons are Raman-active. For n-type GaN with $10^{17} \text{ cm}^{-3} < n < 10^{20} \text{ cm}^{-3}$ the LO phonon couples to the electron plasmon to form a coupled plasmon-LO phonon mode (CPLOM). The CPLOM of n-GaN has two peaks, L^- and L^+ , that can be observed in Raman scattering. Their position and lineshape are in agreement with the standard CPLOM theory [5,6], particularly when a correction for the charge-density mechanism is included [4]. In a recent Raman study of n-InN by Inushima *et al.* [7] it was shown that a CPLOM does not form for free electron concentrations between 10^{18} cm^{-3} and 10^{19} cm^{-3} . Instead, it was reported that the $A_1(\text{LO})$ phonon and the free carriers couple non-linearly, leading to a Fano-like lineshape and a quasicontinuous background scattering. Similar results were reported by Thakur *et al.* [8] and interpreted in terms of Landau damping of the electron plasmon and the coupling of the phonon to electron-hole pair excitations. There are also reports [7,9] indicating that the relative Raman scattering intensity of the LO phonon relative to E_2 increases with decreasing laser energy in the range from 2.54 to 1.49 eV.

Here we investigate the coupling of the $A_1(\text{LO})$ phonon to free electrons in $\text{In}_x\text{Ga}_{1-x}\text{N}$ alloys via Raman scattering using a range of laser excitation energies. It might be expected that at a sufficiently small value of x $\text{In}_x\text{Ga}_{1-x}\text{N}$ would behave more like

GaN (i.e., a CPLOM would be formed) than like InN. Instead, we find no evidence of a CPLOM down to $x = 0.37$. We also find strong resonant Raman scattering of the LO phonon relative to E_2 for laser excitation above the bandgap. Finally, multiphonon Raman scattering of up to 5 LO phonons is observed in $\text{In}_{0.37}\text{Ga}_{0.63}\text{N}$.

EXPERIMENTAL

Epitaxial InGaN films were grown on the c-plane of sapphire substrates with a GaN buffer layer by molecular beam epitaxy [10,11]. Film composition was determined by x-ray diffraction (XRD) and Rutherford backscattering spectrometry (RBS). The value of the energy gap E_g was determined by optical absorption. With one exception, the nominally undoped films had electron concentrations as measured by Hall effect in below $2 \times 10^{18} \text{ cm}^{-3}$ range. Si doping was used to make InN films with electron concentrations up to $5 \times 10^{20} \text{ cm}^{-3}$. We have shown elsewhere that energetic particle irradiation can be used to precisely control the electron concentration in InGaN films through the introduction of native donor defects [12,13]. Here 2 MeV He^+ irradiation at doses up to $9 \times 10^{15} \text{ cm}^{-2}$ was used to raise the electron concentration into the $10^{19} - 10^{20} \text{ cm}^{-3}$ range. Sample parameters are listed in Table 1.

Raman spectroscopy was performed at room temperature in a quasi backscattering geometry using lines of either an Argon ion laser (2.41 – 2.71 eV) or a HeNe laser (1.96 eV) as an excitation source. The collected light was not analyzed for polarization. Data were collected with either a double spectrometer with a photon-counting PMT, a single spectrometer with a holographic laser line filter and a cooled CCD, or a triple spectrometer with a cooled CCD. Spectra collected with different power densities

(achieved by using either a point or line focus) were used to establish that the reported spectra are not affected by photogenerated carriers.

RESULTS

Figure 1 shows Raman spectra obtained with 2.54 eV excitation for a number of undoped $\text{In}_x\text{Ga}_{1-x}\text{N}$ films. For $x = 1$ (InN), two features are observed at 490 and 584 cm^{-1} . Following Inushima *et al.* [7], who obtained similar spectra for InN, the peaks are assigned to the E_2 and $A_1(\text{LO})$ phonons, respectively. As x is decreased to 0.37, both peaks continue to be observed and shift to higher frequency with decreasing x . Notably, the relative intensity of the $A_1(\text{LO})$ phonon peak increases with respect to that of the E_2 phonon for increasing Ga content. Figure 2 shows the Raman spectra of two films with $x = 0.57$ and 0.37 obtained at different laser excitation energies from 2.41 – 2.71 eV. The relative height of the $A_1(\text{LO})$ phonon clearly increases with decreasing laser energy. Figure 3 shows the intensity of the LO phonon scattering normalized to the height of the E_2 phonon graphed vs. $E_{\text{laser}} - E_g$ for all of the films in examined in this study (data for InN from Inushima *et al.* [7] is also included). The relative $A_1(\text{LO})$ intensity clearly increases as the laser excitation approaches the $\text{In}_x\text{Ga}_{1-x}\text{N}$ direct bandgap. The largest value shown in Fig. 3 is for $\text{In}_{0.37}\text{Ga}_{0.63}\text{N}$ ($E_g = 1.9$ eV) excited at 2.41 eV. Figure 4 shows a Raman spectrum obtained for this film using excitation very close to the band edge (1.96 eV). The $A_1(\text{LO})$ peak is observable even against a strong photoluminescence background, although in this case the E_2 phonon could not be observed so that relative intensity could not be quantified.

The effect of the free electron concentration on the Raman spectra of $\text{In}_x\text{Ga}_{1-x}\text{N}$ was also investigated. Figures 5(b) and (c) show spectra from two alloy films in which

the electron concentration has been increased by He^+ irradiation. Also shown in Fig. 5(a) are spectra from Si-doped and He^+ -irradiated InN films that have approximately the same electron concentration. The spectra are normalized to the height of the E_2 phonon peak. The relative height of the $A_1(\text{LO})$ phonon increases with increasing electron concentration in most cases; its frequency also decreases slightly.

The positions of the E_2 and $A_1(\text{LO})$ peaks observed for all of the undoped films in this study are graphed in Fig. 6 as a function of x . Correia *et al.* [14] have reported one-mode behavior for the $A_1(\text{LO})$ phonons for $x < 0.3$ (that is, for Ga-rich InGaN). The present data is consistent with a one-mode behavior for both E_2 and $A_1(\text{LO})$. Most of the observed frequencies for the $A_1(\text{LO})$ phonon are close to what would be expected from a linear extrapolation between the values for InN and GaN, although for $x = 0.5$ and 0.37 , the values are somewhat higher. Finally, for InGaN films with x in the range of $0.4 - 0.5$, strong multiphonon resonant Raman scattering was observed. As shown in Fig. 7, multiphonon LO scattering of up to 5LO is observed in the Raman spectrum of $\text{In}_{0.37}\text{Ga}_{0.63}\text{N}$.

DISCUSSION

The results for InN films with low electron concentrations ($\leq 10^{18} \text{ cm}^{-3}$) and high electron mobilities ($>1000 \text{ cm}^2 \text{ V}^{-1} \text{ s}^{-1}$) shown in Figs. 1 and 5(a) are qualitatively similar to those reported by Inushima *et al.* [7] and Thakur *et al.* [8]. That is, a blue-shifted L^+ peak, as would be predicted from coupling of the LO phonon and the electron plasmon by the standard theory [5] is not observed. Also, the position of the $A_1(\text{LO})$ peak does not shift significantly with electron concentration. It is also clear that a blue-shifted L^+ peak is also not observed for an undoped $\text{In}_{0.85}\text{Ga}_{0.15}\text{N}$ film with a mobility of $1000 \text{ cm}^2 \text{ V}^{-1} \text{ s}^{-1}$

(Fig. 1). For the lower mobility films used in the study (i.e. for $x > 0.7$), the electron plasma would be expected to be heavily damped. In this case, a single coupled CPLOM is predicted to occur. As the electron concentration (or, equivalently, the plasmon frequency ω_p) increases, the coupled mode frequency is predicted to first increase slightly, then decrease and become equal to ω_{LO} at $\omega_p \approx \omega_{LO}$, and finally approach ω_{LO} at very high electron concentrations [6]. This behavior has been observed previously in p-type GaAs [15,16]. The coupled mode is also predicted to be significantly broadened compared to that of the bare LO phonon. As shown in Fig. 5(b)-(c), the $A_1(\text{LO})$ phonon as observed in Raman scattering neither significantly changes its position nor shape as the electron concentration is increased from the mid- 10^{18} cm^{-3} to 2.5×10^{20} for $x = 0.68$ and $3 \times 10^{19} \text{ cm}^{-3}$ for $x = 0.37$. We conclude that the LO phonon does not couple directly to the electron plasmon in these cases, as well.

We are aware of two theoretical treatments of LO phonon scattering in InN. In the study of Inushima *et al.* [7], it was observed that the shape of the $A_1(\text{LO})$ phonon peak was slightly asymmetric to higher frequency and shifted to lower frequency by 3–5 cm^{-1} as n was increased. These effects were interpreted in terms of a Fano resonance between the $A_1(\text{LO})$ phonon and free carriers. Another interpretation has been provided by Thakur *et al.* [8]. In this treatment, it is proposed that the electron plasmon is Landau-damped and that the scattering near the LO phonon frequency is due to \mathbf{q} -dependent coupling of the LO phonon to electron-hole pair excitations. A peak at the LO phonon frequency with an increasing asymmetry to lower frequency is predicted as n increases.

For the InGaN films studied here with 2.54 eV excitation (Fig. 5), the $A_1(\text{LO})$ phonon peak is somewhat asymmetric to lower frequency and increasing the electron

concentration causes a slight (ca. $3 - 5 \text{ cm}^{-1}$) shift to lower frequency. The asymmetry is consistent with the treatment of Thakur *et al.* [8] but the small shift is more consistent with Inushima *et al.* [7], although we note that the asymmetry could be due to alloying-induced wavevector nonconservation that allows non-zone-center phonons from the LO branch to be observed. We conclude that our experimental data do not allow us to determine which theoretical treatment is more applicable to model the unusual behavior of the $A_1(\text{LO})$ phonon in $\text{In}_x\text{Ga}_{1-x}\text{N}$ for $0.37 < x < 1$.

Multiphonon scattering has been studied in GaN. Behr *et al.* [17] used excitation energies varying from 0.5 eV below E_g to slightly above it and observed resonance effects for the $E_1(\text{LO})$ and $2E_1(\text{LO})$ phonons. For excitation above the gap, multiphonon scattering up to $m = 4$ was observed and attributed to an outgoing resonance. It should be noted that, while observable, the higher order scattering fell off rapidly with m . As shown in Fig. 3, resonant scattering of the $A_1(\text{LO})$ phonon at the fundamental band gap in $\text{In}_x\text{Ga}_{1-x}\text{N}$ is evidently stronger and occurs over a wider energy range.

Strong multiphonon resonance Raman scattering similar to that shown for InGaN in Fig. 7 has been observed in a number of semiconductors. LO phonon overtones have been reported in II-VI compounds such as CdS (up to $m = 9$) [18] and ZnTe (up to $m=7$) [19]. The effect is less strong in III-V compounds studied to date with prior reports of overtones up to $m = 3$ for GaP and InAs [20] ($m = 9$ was observed for GaAs in strong magnetic field [21]). There are a number of theoretical models that describe the resonance effect, which is attributed to electron-phonon coupling via the Fröhlich interaction [20]. We consider our results here using the cascade model for multiphonon resonant Raman scattering originally proposed by Martin and Varma [22]. The steps

involved are: (1) absorption of a laser photon to form an exciton with emission of an LO phonon to conserve center of mass momentum \mathbf{K} ; (2) relaxation of exciton by emission of one or more LO phonons; (3) radiative recombination of exciton with emission of a final LO phonon to conserve \mathbf{K} . Steps 1 and 3 involve virtual intermediate states. The scattering probability for m phonons $P_{ph}^{(m)}$ can, in this model, be written formally in terms of the rate of relaxation of the excitons via emission of one LO phonon, the damping of each exciton state, and the rate of phonon-assisted exciton recombination [23],

$$P_{ph}^{(m)} \propto \alpha_1 \left(\frac{\tau_{rel}}{\Gamma_1(\mathbf{K}_1)} \right) \left(\frac{\tau_{rel}}{\Gamma_1(\mathbf{K}_2)} \right) \cdots \left(\frac{\tau_{rel}}{\Gamma_1(\mathbf{K}_{m-2})} \right) \left(\frac{\tau_{rad}}{\Gamma_1(\mathbf{K}_{m-1})} \right) \quad (1)$$

where α_1 is the absorption coefficient for LO-phonon-assisted formation of excitons (step 1 above), τ_{rel} is the relaxation rate for excitons via emission of one LO phonon, $\Gamma_1(\mathbf{K}_i)$ is the damping of the exciton state $E_1(\mathbf{K}_i)$, and τ_{rad} is the rate of LO-phonon assisted radiative recombination of excitons. Evidently, the relative probabilities of m LO emission compared to $(m-1)$ LO depends on the relative magnitudes of τ_{rel} and $\Gamma_1(\mathbf{K}_i)$.

By making a number of simplifying assumptions Zeyher [24] was able to predict the relative intensities of phonons above $m = 2$ in this model. The assumptions are: (1) infinite hole mass, (2) neglect of the momentum dependence of the electron-phonon interaction, and (3) neglect of momentum dependence of the LO phonon frequency. In this formulation, the relative scattering intensity for m LO is

$$\frac{d\sigma}{d\Omega} = \sigma_0 \frac{D^m}{m^2} \int_0^\infty y^{2-m} \left[\prod_{i=1}^{m-1} F_{ii}(y) \right] \left[\sum_{i=0,m; j=0,m} (-1)^{(i+j)/m} F_{ij}(y) \right] dy, \quad (2)$$

where the double sum is just over 0 and m , and

$$F_{ij}(y) = i \log \left(\frac{y - \sqrt{z_i^*} + \sqrt{z_j}}{-y - \sqrt{z_i^*} + \sqrt{z_j}} \right), \quad (3)$$

$$z_i = \frac{\hbar\omega_{laser} - i\eta(\omega') - E_g - j\hbar\Omega}{\hbar\Omega}, \quad (4)$$

$$\eta(\omega') = 2D\hbar\Omega \left(\frac{\hbar\omega' - E_g - \hbar\Omega}{\hbar\Omega} \right)^{1/2} \Theta \left(\frac{\hbar\omega' - E_g - \hbar\Omega}{\hbar\Omega} \right) + \eta_0, \quad (5)$$

$$\text{and } D = \frac{C^2(1+f)}{8\pi^2\Omega^2}. \quad (6)$$

In the equations above y is a normalized momentum difference, z is the exciton self energy normalized to the LO phonon energy, $\omega' = \hbar\omega_{laser} - j\hbar\Omega$, f is the Bose-Einstein distribution function for phonons, and C is the electron phonon interaction constant. The step function Θ in the damping term $\eta(\omega')$ reflects the fact that an exciton with an energy less than $\hbar\Omega$ above the resonance at E_g cannot relax by emission of an LO phonon with frequency Ω and will relax at a (lower) rate η_0 .

The adjustable parameters in the model are η_0 , the off-resonance exciton coupling to phonons, and C , the electron-phonon coupling parameter. We assumed a value for η_0 of $0.01\hbar\Omega$ as had been used for the modeling of II-VI semiconductors and a value for C of 0.15 eV. Strong multiphonon emission is only observed for $D > 0.1$. For the values assumed here $D = 0.12$ at 300 K. As shown in Fig. 8, the model is in reasonable agreement with the data for the three laser energies used. We note that this modeling is not applicable for the GaN multiphonon scattering reported by Behr et al. [17] because $E_{laser} - n\Omega_{LO} < E_g$ for $m > 2$ (that is, a cascade mechanism was not possible).

As a final note, it should be stated that the strong resonant Raman scattering observed here would suggest that there is a relatively strong electron-phonon interaction in InN and In-rich InGaN. On the other hand, in order to understand the first order $A_1(\text{LO})$ Raman spectrum, it must be assumed that the LO phonon does not couple directly to the electron plasmon. There is other experimental evidence that the electron-phonon coupling in InN may be fairly weak. Subpicosecond differential transmission measurements have been interpreted in terms of a weak carrier-LO phonon interaction [25] and transient Raman measurements have been used to show that the electron saturation drift velocity in InN is $2 \times 10^8 \text{ cm s}^{-1}$, significantly higher than in other III-V semiconductors [26]. The key to resolving this apparent contradiction may lie in distinguishing the interactions of electrons high in the conduction band (those involved in the multiphonon cascade process) from those nearer to the bottom of the conduction band.

CONCLUSIONS

Resonance Raman effects in $\text{In}_x\text{Ga}_{1-x}\text{N}$ epitaxial films with $0.37 < x < 1$ were studied. In contrast to GaN, free carriers in $\text{In}_x\text{Ga}_{1-x}\text{N}$ with $x > 0.37$ do not form a coupled plasmon-LO phonon mode (CPLOM). Instead, the $A_1(\text{LO})$ phonon appears to interact with the carriers through a weaker mechanism similar to that observed in InN. A strong, broad resonance in the LO phonon scattering efficiency and also multiphonon scattering is observed with excitation above the bandgap. For $\text{In}_{0.37}\text{Ga}_{0.63}\text{N}$, LO phonon overtones up to $m = 5$ are observed; this is the highest value of m reported for multiphonon scattering in a III-V compound under ambient conditions.

ACKNOWLEDGMENTS

This work was supported by the Director's Innovation Initiative Program, National Reconnaissance Office and by the Director, Office of Science, Office of Basic Energy Sciences, Division of Materials Sciences and Engineering, of the U.S. Department of Energy under Contract No. DE-AC02-05CH11231. The work at Cornell University was supported by ONR under Contract No. N000149910936.

TABLE 1. Direct band gaps, electron concentrations, and mobilities measured for the InGaN films used in this study.

Film	E_g (eV)	n (cm ⁻³)	μ (cm ² V ⁻¹ s ⁻¹)
<i>undoped</i>			
InN	0.7	1×10^{18}	1560
InN	0.7	7×10^{17}	1290
In _{0.85} Ga _{0.15} N	0.8	1.4×10^{18}	700
In _{0.68} Ga _{0.32} N	1.1	2×10^{18}	40
In _{0.57} Ga _{0.43} N	1.5	2.5×10^{19}	32
In _{0.37} Ga _{0.63} N	1.9	1×10^{18}	20
<i>alpha-irradiated</i>			
InN		1.7×10^{20}	90
In _{0.68} Ga _{0.32} N		2×10^{18}	30
In _{0.37} Ga _{0.63} N		3×10^{19}	8.6
<i>Si doped</i>			
InN		2×10^{20}	110

-
1. V. Yu. Davydov, A. A. Klochikhin, R. P. Seisyan, V. V. Emtsev, S. V. Ivanov, F. Bechstedt, J. Furthmüller, H. Harima, A. V. Murdryi, J. Aderhold, O. Semchinova, and J. Graul, *Phys. Stat. Sol. (b)* **229**, R1 (2002).
 2. J. Wu, W. Walukiewicz, K. M. Yu, J. W. Ager III, E. E. Haller, H. Lu, W. J. Schaff, Y. Saito, and Y. Nanishi, *Appl. Phys. Lett.* **80**, 3967 (2002).
 3. K. Sugita, H. Takatsuka, A. Hashimoto, and A. Yamamoto, *Phys. Stat. Sol. (b)* **240**, 421 (2003).
 4. H. Harima, *J. Phys. Condens. Matter* **14**, R967 (2002).
 5. G. Irmer, V. V. Toporov, B. H. Bairamov, and J. Monecke, *Phys. Status Solidi b* **119**, 595 (1983) and references therein.
 6. G. Irmer, M. Wenzel, and J. Monecke, *Phys. Rev. B* **56**, 9524 (1997).
 7. T. Inushima, M. Higashiwaki, and T. Matsui, *Phys. Rev. B* **68**, 235204 (2003).
 8. J. S. Thakur, D. Haddad, V. M. Naik, R. Naik, G. W. Auner, H. Lu, and W. J. Schaff, *Phys. Rev. B* **71**, 115203 (2005).
 9. M. Kuball, J. W. Pomeroy, M. Wintrebert-Fouquet, K. S. A. Butcher, H. Lu, and W. J. Schaff, *J. Crystal Growth* **269**, 59 (2004).
 10. H. Lu, William J. Schaff, Jeonghyun Hwang, Hong Wu, Wesley Yeo, Amit Pharkya, and Lester F. Eastman, *Appl. Phys. Lett.* **77**, 2548-2550 (2000).
 11. H. Lu, Schaff, W.J.; Jeonghyun Hwang; Hong Wu; Koley, G.; Eastman, L.F. Source, *Appl. Phys. Lett.* **79** 1489-91 (2001).

-
12. J. Wu, W. Walukiewicz, W. Shan, K.M. Yu, W. Shan, J. W. Ager III, E. E. Haller, H. Lu, and W. J. Schaff, W. K. Metzger, S. R. Kurtz, J. F. Geisz, *J. Appl. Phys.* **94**, 6477-82 (2003).
 13. S. X. Li, K. M. Yu, J. Wu, R. E. Jones, W. Walukiewicz, J. W. Ager III, W. Shan, E. E. Haller, H. Lu, and W. J. Schaff, *Phys. Rev. B* **71**, 161201(R) (2005).
 14. M. R. Correia, S. Pereira, E. Pereira, J. Frandon, and E. Alves, *Appl. Phys. Lett.* **83**, 4761 (2003).
 15. K. Wan and J. F. Young, *Phys. Rev. B* **41**, 10772 (1990).
 16. F. Fukasawa and S. Perkowitz, *Phys. Rev. B* **50**, 14119 (1994).
 17. D. Behr, J. Wagner, J. Schneider, H. Amano, and I. Akasaki, *Appl. Phys. Lett.* **68**, 2404 (1996).
 18. J. F. Scott, R. C. C. Leite, and T. C. Damen, *Phys. Rev.* **188**, 1285 (1969); M. V. Klein and S. P. S. Porto, *Phys. Rev. Lett.* **22**, 782 (1969).
 19. A. A. Klochikhin, Y. V. Morozenko, and S. A. Permogorov, *Sov. Phys. Solid State* **20**, 2057 (1978).
 20. M. Cardona, *Resonance Phenomenon*, in *Light Scattering in Solids II*, eds. M. Cardona and G. Güntherodt (Springer, Berlin, 1982), pp. 145-151, 167-172 and references therein.
 21. T. Ruf and M. Cardona, *Phys. Rev. Lett.* **63**, 2288 (1989).
 22. R. M. Martin and C. M. Varma, *Phys. Rev. Lett.* **26**, 1241, 1971
 23. P. Y. Yu and M. Cardona, *Fundamentals of Semiconductors, 3rd Edition*, (Springer, Berlin, 2001), pp. 413-416.

24. R. Zeyher, *Solid State Commun.* **16**, 49 (1975).
25. F. Chen, A. N. Cartwright, H. Lu, and W. J. Schaff, *Appl. Phys. Lett.* **83**, 4985 (2003).
26. K. T. Tsen, C. Poweleit, D. K. Ferry, H. Lu, and W. J. Schaff, *Appl. Phys. Lett.* **86**, 222103 (2005).

FIGURE CAPTIONS

Fig. 1. Room temperature Raman spectra of $\text{In}_x\text{Ga}_{1-x}\text{N}$ films obtained with 488 nm (2.54 eV) excitation at 300 mW. Spectra are normalized to the height of the E_2 phonon and offset for clarity

Fig. 2. Raman spectra of $\text{In}_x\text{Ga}_{1-x}\text{N}$ films obtained with 2.41 – 2.71 eV laser excitation: (a) $x = 0.37$, $E_g = 1.9$ eV; (b) $x = 0.57$, $E_g = 1.7$ eV. Spectra are normalized to the height of the E_2 phonon peak.

Fig. 3. Height of LO phonon peak normalized to height of E_2 phonon peak for Raman spectra of $\text{In}_x\text{Ga}_{1-x}\text{N}$ ($0.37 < x < 1$) as a function of laser excitation relative to the direct gap of the material. Dotted lines connect points for the same sample and are guides to the eye. Literature data for InN from reference 7 are also shown.

Fig. 4. Raman spectrum of $\text{In}_{0.37}\text{Ga}_{0.63}\text{N}$ ($E_g = 1.9$ eV) obtained with 632.8 nm (1.96 eV) excitation. The resonance-enhanced $A_1(\text{LO})$ phonon is observed in spite of a large background due to band edge photoluminescence. The absolute energy scale is shown as the top axis.

Fig. 5. Raman spectra of (a) InN, (b) $\text{In}_{0.68}\text{Ga}_{0.32}\text{N}$, and (c) $\text{In}_{0.37}\text{Ga}_{0.63}\text{N}$ as a function of electron concentration (the increased electron concentration is produced by 2 MeV He^+ irradiation, see text). A heavily Si-doped InN film is also shown in (a).

Fig. 6. Frequencies of E_2 and $A_1(\text{LO})$ phonons as a function of x . Data for the $A_1(\text{LO})$ phonon from Ga-rich InGaN films from ref. 14 is also shown (filled triangles). Linear extrapolations between endpoint values (InN and GaN) of 490 cm^{-1} and 570 cm^{-1} for E_2 and 590 and 735 cm^{-1} for $A_1(\text{LO})$ are shown with dotted lines.

Fig. 7. Multiphonon Raman scattering observed in $\text{In}_{0.37}\text{Ga}_{0.63}\text{N}$ ($E_g = 1.9$ eV) for three different laser excitation energies. Observed phonon energies are indicated for 2.71 eV excitation; LO overtones up to 5LO are observed. The rising background to lower energy is photoluminescence. Spectra are normalized to the incident laser power, which was in the 100-300 mW range, and are offset for clarity.

Fig. 8. Experimental LO phonon intensities for multiphonon resonance Raman scattering in $\text{In}_{0.37}\text{Ga}_{0.63}\text{N}$ ($E_g = 1.9$ eV) obtained at the three indicated laser energies. The intensity of the m th LO Raman peak is normalized to $m = 2$. The x-axis is the energy of the m th phonon overtone relative to E_g normalized by the phonon energy. Dotted lines are the predictions of the model of Zeyher [24] using the parameters discussed in the text; the theory does not consider the $m=1$ case but the experimental data are shown for completeness.

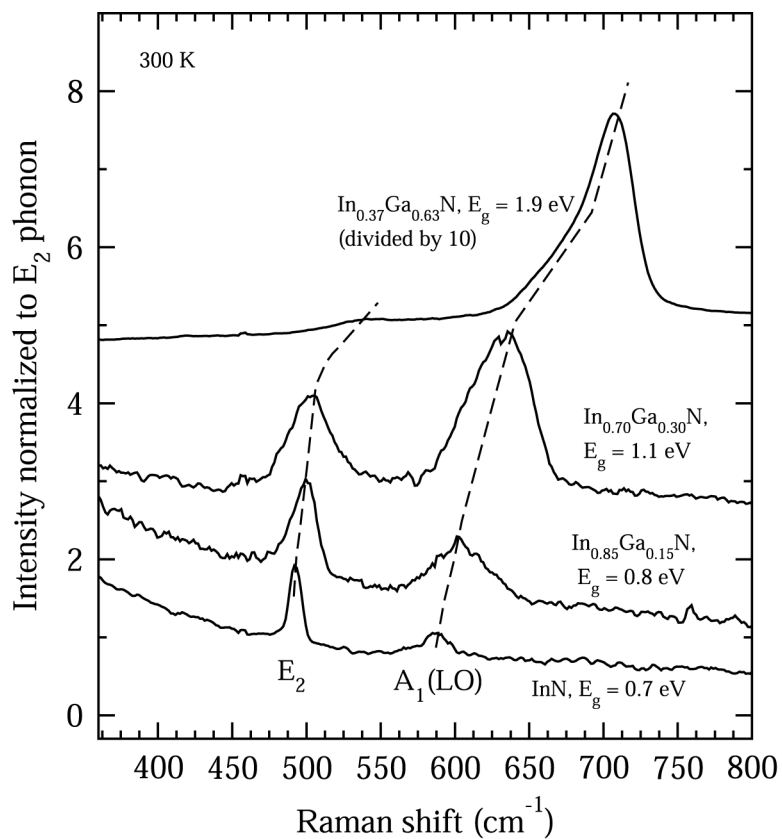


Fig. 1. Room temperature Raman spectra of $\text{In}_x\text{Ga}_{1-x}\text{N}$ films obtained with 488 nm (2.54 eV) excitation at 300 mW. Spectra are normalized to the height of the E_2 phonon and offset for clarity

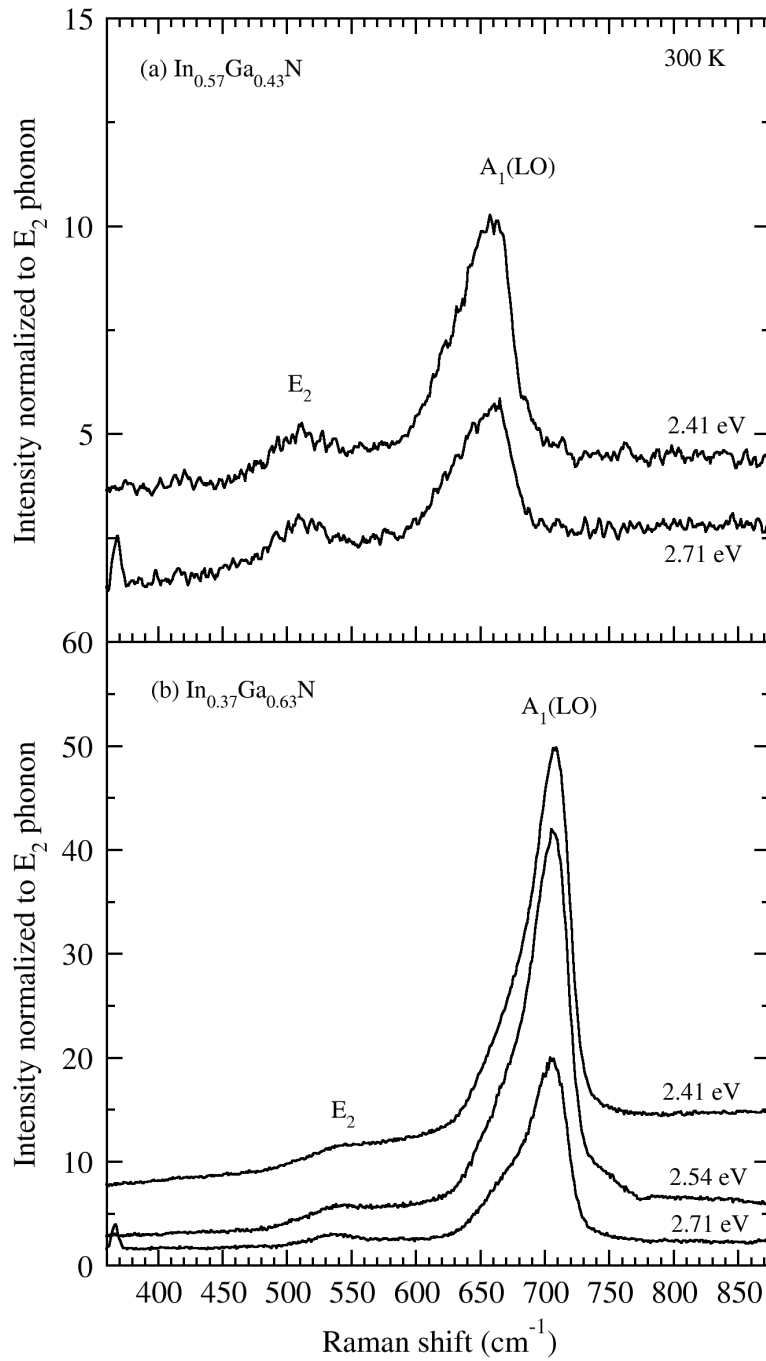


Fig. 2. Raman spectra of In_xGa_{1-x}N films obtained with 2.41 – 2.71 eV laser excitation:

(a) $x = 0.37$, $E_g = 1.9$ eV; (b) $x = 0.57$, $E_g = 1.7$ eV.

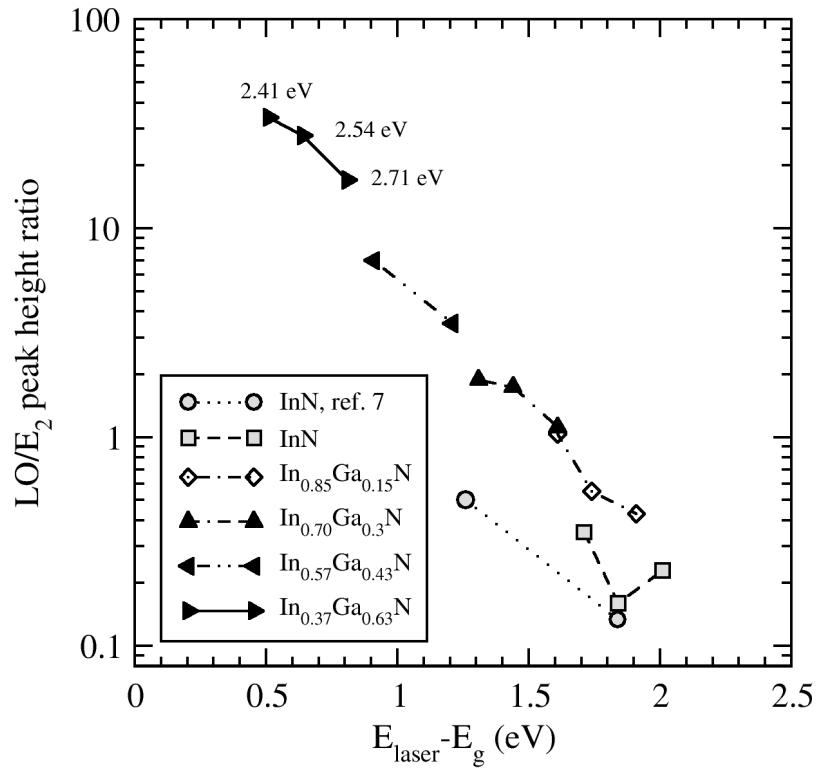


Fig. 3. Height of LO phonon peak normalized to height of E_2 phonon peak for Raman spectra of $\text{In}_x\text{Ga}_{1-x}\text{N}$ ($0.37 < x < 1$) as a function of laser excitation relative to the direct gap of the material. Dotted lines connect points for the same sample and are guides to the eye. Literature data for InN from reference 7 are also shown.

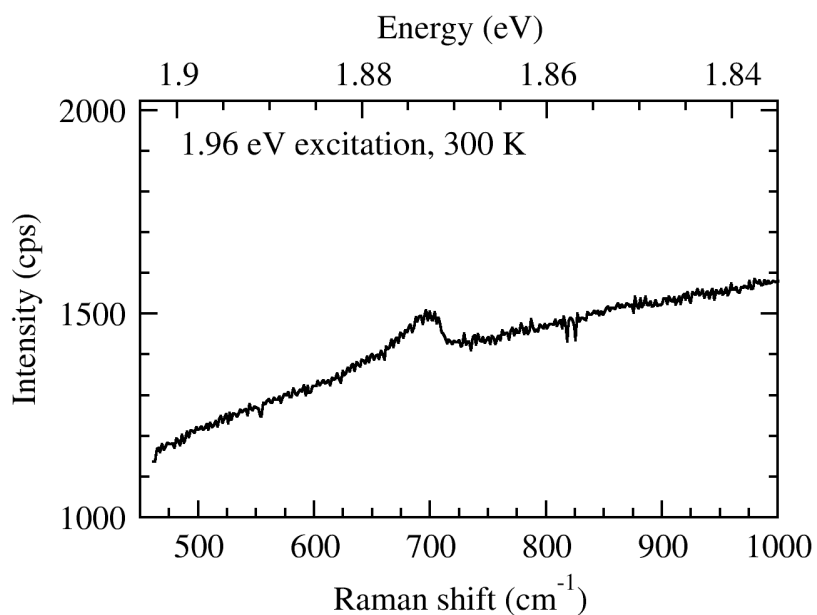


Fig. 4. Raman spectrum of $\text{In}_{0.37}\text{Ga}_{0.63}\text{N}$ ($E_g = 1.9$ eV) obtained with 632.8 nm (1.96 eV) excitation. The resonance-enhanced $A_1(\text{LO})$ phonon is observed in spite of a large background due to band edge photoluminescence.

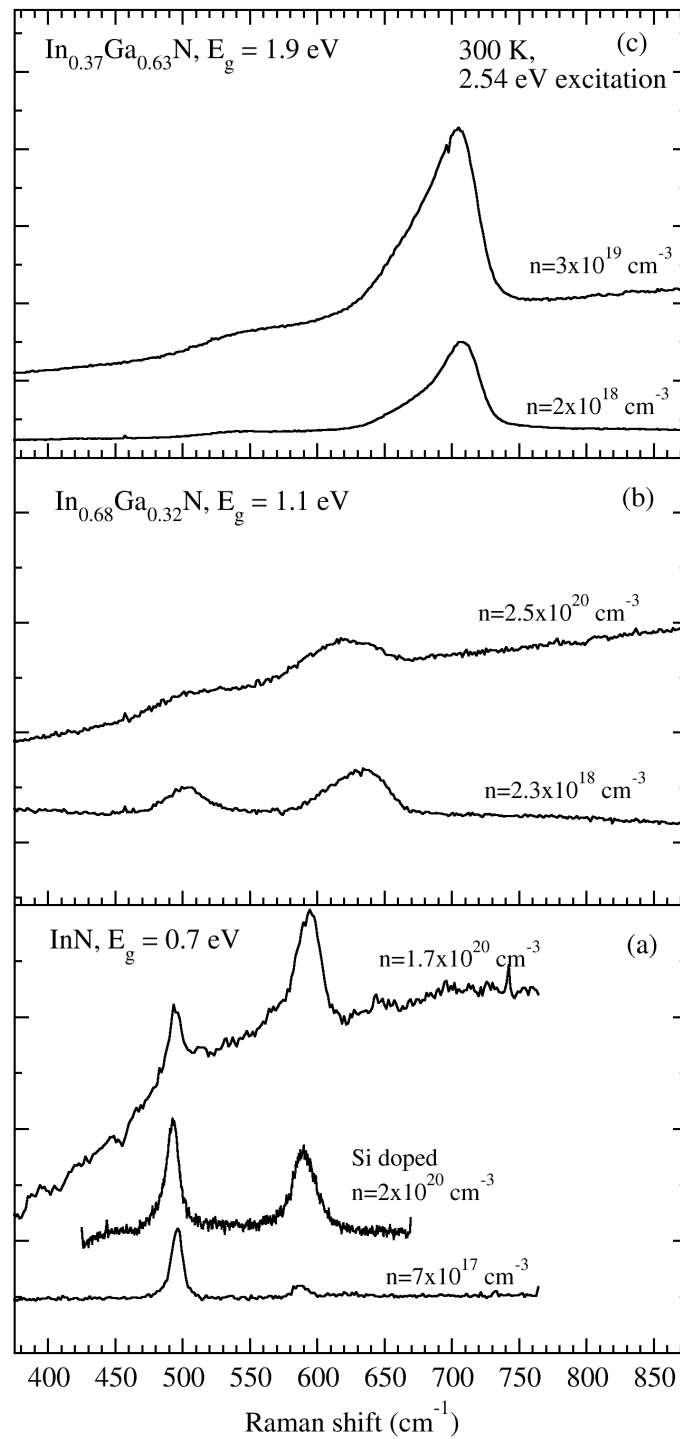


Fig. 5. Raman spectra of (a) InN, (b) $\text{In}_{0.68}\text{Ga}_{0.32}\text{N}$, and (c) $\text{In}_{0.37}\text{Ga}_{0.63}\text{N}$ as a function of electron concentration (the increased electron concentration is produced by 2 MeV He^+ irradiation, see text). A heavily Si-doped InN film is also shown in (a).

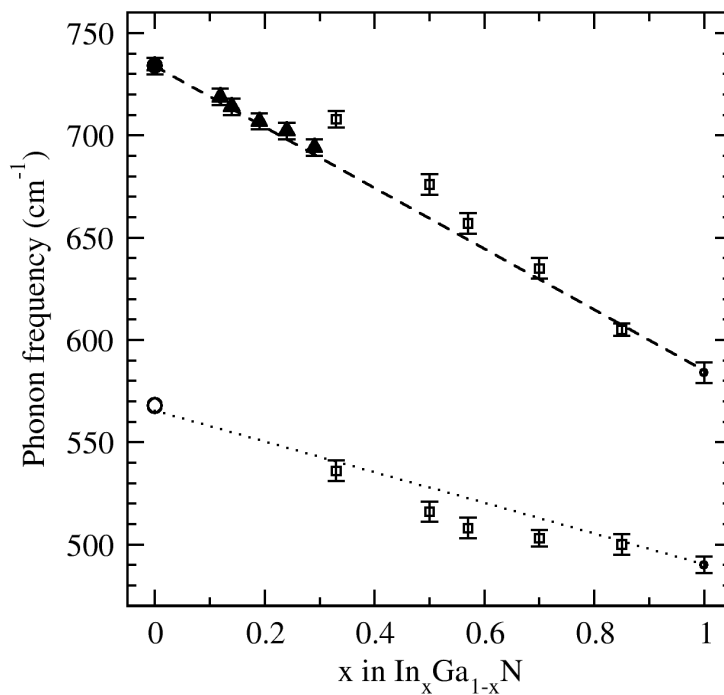


Fig. 6. Frequencies of E_2 and $A_1(\text{LO})$ phonons as a function of x . Data for the $A_1(\text{LO})$ phonon from Ga-rich InGaN films from ref. 14 is also shown (filled triangles). Linear extrapolations between endpoint values (InN and GaN) of 490 cm^{-1} and 570 cm^{-1} for E_2 and 590 and 735 cm^{-1} for $A_1(\text{LO})$ are shown with dotted lines.

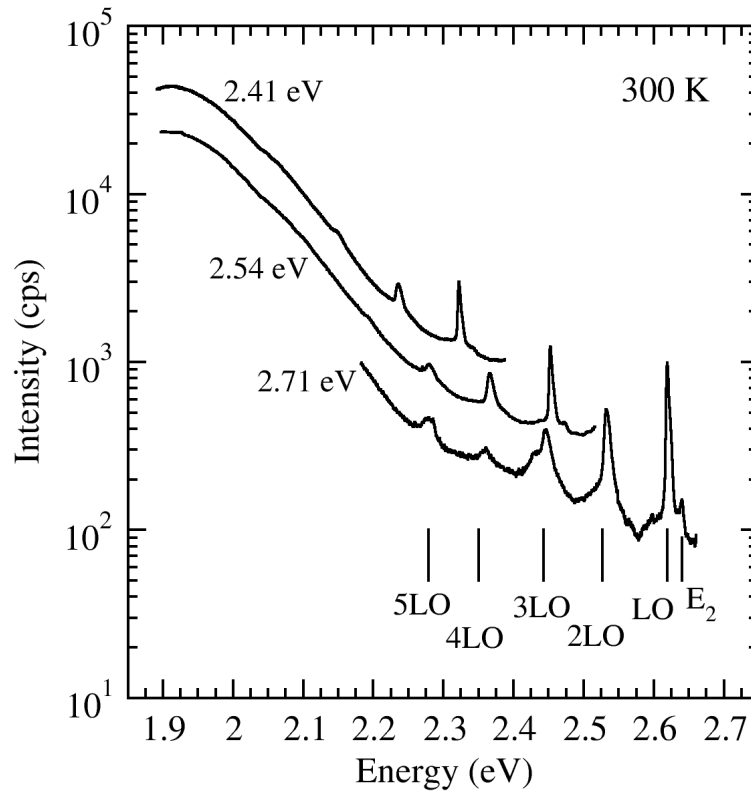


Fig. 7. Multiphonon Raman scattering observed in $\text{In}_{0.37}\text{Ga}_{0.63}\text{N}$ ($E_g = 1.9$ eV) for three different laser excitation energies. Observed phonon energies are indicated for 2.71 eV excitation; LO overtones up to 5LO are observed. The rising background to lower energy is photoluminescence. Spectra are normalized to the incident laser power, which was in the 100-300 mW range, and are offset for clarity.

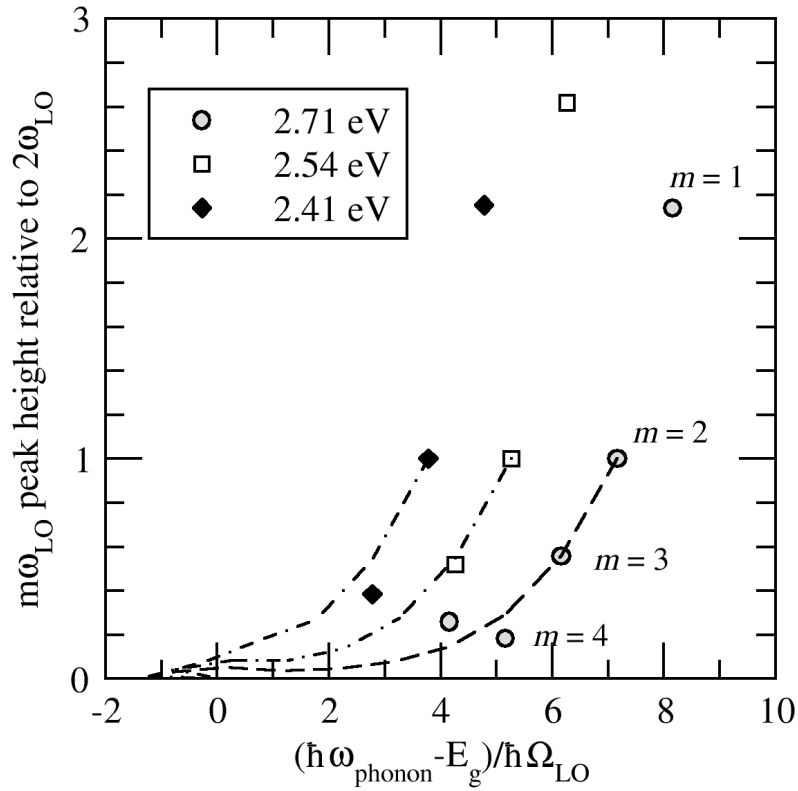


Fig. 8. Experimental LO phonon intensities for multiphonon resonance Raman scattering in $\text{In}_{0.37}\text{Ga}_{0.63}\text{N}$ ($E_g = 1.9$ eV) obtained at the three indicated laser energies. The intensity of the m th LO Raman peak is normalized to $m = 2$. The x-axis is the energy of the m th phonon overtone relative to E_g normalized by the phonon energy. Dotted lines are the predictions of the model of Zeyher [24] using the parameters discussed in the text; the theory does not consider the $m=1$ case but the experimental data are shown for completeness.